

Mechanistic Insights on the Copolymerization of Polar Vinyl Monomers with Neutral Ni(II) Catalysts

Andreas Berkefeld, Matthias Drexler, Heiko M. Möller, and Stefan Mecking*

Chemical Materials Science, Department of Chemistry, University of Konstanz,
Universitätsstrasse 10, D-78457 Konstanz, Germany

Received February 27, 2009; E-mail: stefan.mecking@uni-konstanz.de

Abstract: The Ni(II) complexes [(N \wedge O)Ni(H)(PMe₃)] (**1**) and [(N \wedge O)Ni(CH₂CH₃)(dmsO)] (**3**) (N \wedge O = κ^2 -{(2,6-(3,5-(F₃C)₂C₆H₃)₂C₆H₃)-N=C(H)-(3,5-I₂-2-O-C₆H₂)}) were found to be well-defined model compounds to study the reactivity of polymerization active neutral Ni(II) species toward polar vinyl monomers. Methyl acrylate (MA) insertion into the Ni(II)–hydride bond of **1** was monitored at $T \geq -40$ °C by NMR spectroscopy. 2,1-Insertion yields the functionalized Ni(II) alkyl complex [(N \wedge O)Ni(C α H(CH₃)C β (O)OCH₃)(PMe₃)] (**4**). Low-temperature 2D ROESY data indicate a weak Ni(II)···O=C β interaction in **4**. This is supported by ab initio calculations at the gradient-corrected DFT (BP86/LACPV*) level of theory. Exposure of **1** to equal amounts of MA and ethylene afforded **4** and the Ni(II) ethyl complex **7** in a 9:1 ratio, which indicates that MA and ethylene effectively compete with each other for coordination and insertion. NMR spectroscopic monitoring revealed that **4** is stable in the absence of residual **1** at low temperatures but is subject to rapid bimolecular elimination of the functionalized alkyl moiety in the presence of free Ni(II) hydride species even at $T = -40$ °C. Isomerization into the 1,2-MA-insertion product was observed at $T = 25$ °C but occurred slowly compared to decomposition, which occurs at 0 °C by reaction of **4** with Ni(II) hydride formed by β -elimination from **4** itself at this temperature. Exposure of the higher Ni(II) alkyl complex **3** to MA in the presence of excess ethylene results in the immediate formation of methyl pentanoate as the ultimate decomposition product. Functionalized Ni(II) alkyl species formed from 2,1-insertion of MA into the metal–carbon bond of higher Ni(II) alkyls are subject to rapid hydrolysis in the presence of trace amounts of water in the reaction medium, which contrasts the stability of nonfunctionalized Ni(II) alkyls toward water. Exposure of **1** to vinyl acetate (VA) affords the kinetic 1,2-insertion product [(N \wedge O)Ni(CH₂CH₂OC γ (O)CH₃)(PMe₃)] (**5**) at temperatures $T \geq -10$ °C, which rearranges into the thermodynamically favored 2,1-insertion product [(N \wedge O)Ni(CH(CH₃)OC(O)CH₃)(PMe₃)] (**6**). NMR data and ab initio calculations suggest a Ni(II)···O=C γ interaction in **6**. **5** decomposes via β -acetate elimination to yield ethylene and Ni(II) acetate species. Notably, VA does not undergo observable nickel–carbon bond insertion with **3**, but reacted with Ni(II) hydride species in equilibrium with **3** to yield **5*** which is subject to rapid decomposition via β -acetate elimination.

Introduction

Insertion polymerization of ethylene and propylene, initiated by the seminal findings of Ziegler¹ and Natta,² is applied today on a vast industrial scale. By contrast, an insertion (co)polymerization of electron-deficient vinyl monomers, such as acrylates, had remained elusive for a long time. It was not until the mid 1990s that cationic Pd(II) diimine complexes were reported to catalyze the insertion copolymerization of ethylene and 1-olefins with acrylates.³ These d⁸-metal (late transition metal) complexes are less oxophilic by comparison to early transition metal polymerization catalysts, and therefore more tolerant toward polar moieties.⁴ In-depth NMR spectroscopic studies revealed that κ^2 -C,O-coordinate Pd(II) alkyl species [(diimine)Pd(κ^2 -

CHRCH₂CH₂C(O)OCH₃)]⁺ (R = growing polymer chain) are formed by chelating coordination of the carbonyl group of an inserted methyl acrylate (MA) unit. Opening of these chelates by coordination of incoming monomer to form the corresponding olefin complexes is the turnover-limiting step during copolymer chain-growth.^{3,5} While the copolymers obtained with cationic Pd(II) diimine are highly branched due to extensive chain walking, with analogous Ni(II) complexes,⁶ and with neutral Pd(II) phosphinosulfonate complexes, linear ethylene–MA copolymers are formed.⁷ The latter also enable multiple insertions of MA,⁸ and copolymerizations of ethylene even with acrylonitrile.⁹

- (1) (a) Ziegler, K.; Breil, H.; Holzkamp, E.; Martin, H. *DE* 973626, 1953. (b) Ziegler, K.; Holzkamp, E.; Breil, H.; Martin, H. *Angew. Chem.* **1955**, *67*, 426. (c) Ziegler, K.; Holzkamp, E.; Breil, H.; Martin, H. *Angew. Chem.* **1955**, *67*, 541–547.
(2) Natta, G.; Pino, P.; Corradini, P.; Danusso, F.; Mantica, E.; Mazzanti, G.; Moraglio, G. *J. Am. Chem. Soc.* **1955**, *77*, 1708–1710.
(3) (a) Johnson, L. K.; Mecking, S.; Brookhart, M. *J. Am. Chem. Soc.* **1996**, *118*, 267–268. (b) Mecking, S.; Johnson, L. K.; Wang, L.; Brookhart, M. *J. Am. Chem. Soc.* **1998**, *120*, 888–899.

- (4) (a) Ittel, S. D.; Johnson, L. K.; Brookhart, M. *Chem. Rev.* **2000**, *100*, 1169–1203. (b) Gibson, V. C.; Spitzmesser, S. K. *Chem. Rev.* **2003**, *103*, 283–315. (c) Mecking, S. *Coord. Chem. Rev.* **2000**, *203*, 325–351. (d) Mecking, S. *Angew. Chem., Int. Ed.* **2001**, *40*, 534–540. (e) Guan, Z. *Chem.–Eur. J.* **2002**, *8*, 3086–3092. (f) Domski, G. J.; Rose, J. M.; Coates, G. W.; Bolig, A. D.; Brookhart, M. *Prog. Polym. Sci.* **2007**, *32*, 30–92.
(5) Related stoichiometric studies of acrylate insertion in Pd(II) complexes: (a) Braunstein, P.; Frison, C.; Morise, X. *Angew. Chem., Int. Ed.* **2000**, *39*, 2867–9870. (b) Braunstein, P.; Agostinho, M. *Chem. Commun.* **2007**, 58–60.

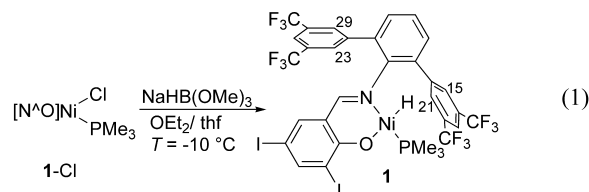
The aforementioned studies have prompted extensive studies of novel neutral nickel(II) olefin polymerization catalysts.¹⁰ By comparison to the aforementioned catalysts, they are much more stable to protic and even aqueous media.^{10f,11–13,15b} At the same time, polymer microstructures and resulting crystallinities and thermal behavior can be varied in a controlled fashion over a wide range via the catalyst. However, despite intense studies of their polymerization properties, to date the copolymerization of ethylene or 1-olefins with polar vinyl monomers, like MA, to high-molecular-weight copolymers employing neutral Ni(II) precatalysts has suffered from either low effectivity or rapid catalyst deactivation.¹⁴ An understanding of the problems

associated with this reaction is desirable. By comparison to the aforementioned cationic Pd(II) complexes, neutral Ni(II) complexes are, unfortunately, less amenable to mechanistic studies via direct observation with NMR spectroscopy.¹⁵ Neutral Ni(II) salicylaldimine catalysts were found to be subject to rapid deactivation in attempted copolymerizations of 1-olefins with polar vinyl monomers. In a study of the organic decomposition products formed by reaction of a salicylaldiminato phenyl complex, [(N \wedge O)Ni(C₆H₅)(PPh₃)] (N \wedge O = κ^2 -{(2,6-(iPr)₂C₆H₃)-N=C(H)-(3-anthryl-2-O-C₆H₂)}), with MA in toluene solution, methyl *trans*-cinnamate and methyl 3-phenylbutanoate were formed over the course of 1 day at 80 °C. Carrying out the reaction in the presence of 2,3,3-*d*₃-MA allowed to trace back the origin of the methylene-hydrogen atoms in the saturated reaction product, which are provided by the substrate itself. Protonation of an intermittent metal alkyl species by free ligand, (N \wedge O)H, formed by reductive elimination from [(N \wedge O)NiH] species, was suggested as a most likely pathway. In addition, hydrolysis of insertion products was identified as a decomposition route.¹⁶

We now report a comprehensive study of the nature and reactivity of neutral Ni(II) alkyl insertion products of acrylate and vinyl acetate, based on direct NMR spectroscopic observations.

Results and Discussion

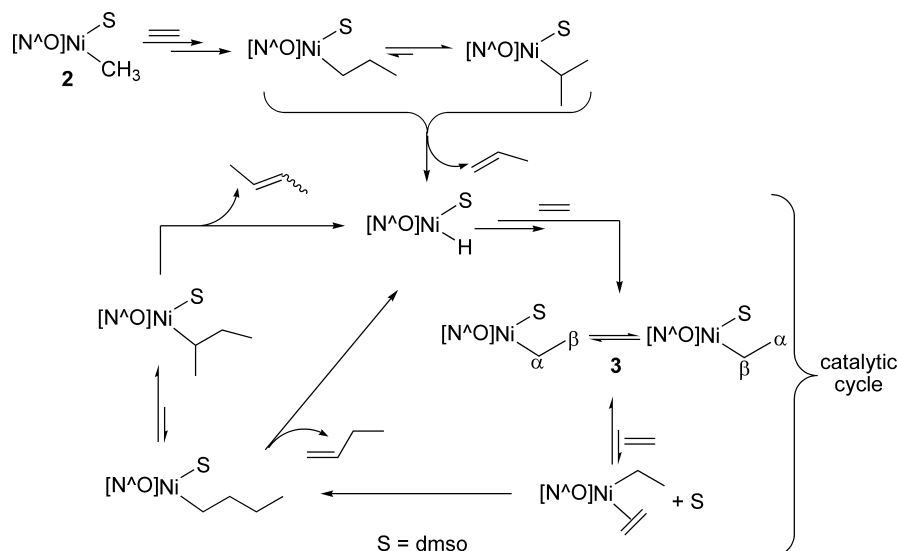
General Considerations. Highly reactive Ni(II) hydride and higher Ni(II) alkyl species [(N \wedge O)NiR(L)] (R = H, CH₃, C₂H₅; L = PMe₃, dmsO) of a salicylaldiminato ligand based on a terphenylamine (N \wedge O; eq 1) were employed as precursors for mechanistic studies. This particular salicylaldimine was chosen because Ni(II) complexes of this ligand are long-lived, robust, and very active catalysts for ethylene polymerization.^{10m,q} The Ni(II) hydride complex **1** was either synthesized on a preparative scale (eq 1) from the corresponding Ni(II) chloride complex **1-Cl** (Figure S1 and Table S1, Supporting Information),^{15b} or generated in situ in thf-*d*₈ solution at low temperatures directly in an NMR tube.



Although the in situ preparation is convenient to generate concentrated solutions of **1** within short times for NMR studies,

- (6) (a) Johnson, L.; Bennett, A.; Dobbs, K.; Hauptman, E.; Ionkin, A.; Ittel, S.; McCord, E.; McLain, S.; Radzewich, C.; Yin, Z.; Wang, L.; Wang, Y.; Brookhart, M. *Polym. Mater. Sci. Eng.* **2002**, *86*, 319. (b) Wang, L.; Hauptman, E.; Johnson, L. K.; Marshall, W. J.; McCord, E. F.; Wang, Y.; Ittel, S. D.; Radzewich, C. E.; Kunitsky, K.; Ionkin, A. S. *Polym. Mater. Sci. Eng.* **2002**, *86*, 322. (c) Johnson, L.; et al. *ACS Symp. Ser.* **2003**, *857*, 131–142.
- (7) (a) Drent, E.; van Dijk, R.; van Ginkel, R.; van Oort, B.; Pugh, R. I. *Chem. Commun.* **2002**, 744–745. Review: (b) Berkefeld, A.; Mecking, S. *Angew. Chem., Int. Ed.* **2008**, *47*, 2538–2542.
- (8) (a) Guironnet, D.; Roesle, P.; Rünzi, T.; Göttker-Schnetmann, I.; Mecking, S. *J. Am. Chem. Soc.* **2009**, *131*, 422–423. Also see, (b) Chen, C.; Luo, S.; Jordan, R. F. *J. Am. Chem. Soc.* **2008**, *130*, 12892–12893.
- (9) Kochi, T.; Noda, S.; Yoshimura, K.; Nozaki, K. *J. Am. Chem. Soc.* **2007**, *129*, 8948–8949.
- (10) (a) Braunstein, P.; Pietsch, J.; Chauvin, Y.; Mercier, S.; Saussine, L.; DeCian, A.; Fischer, J. *J. Chem. Soc., Dalton Trans.* **1996**, 3571–3574. (b) Braunstein, P.; Pietsch, J.; Chauvin, Y.; DeCian, A.; Fischer, J. *J. Organomet. Chem.* **1997**, *529*, 387–393. (c) Wang, C.; Friedrich, S.; Younkin, T. R.; Li, R. T.; Grubbs, R. H.; Bansleben, D. A.; Day, M. W. *Organometallics* **1998**, *17*, 3149–3151. (d) Johnson, L. K.; Bennett, A. M. A.; Ittel, S. D.; Wang, L.; Parthasarathy, A.; Hauptman, E.; Simpson, R. D.; Feldman, J.; Coughlin, E. B. (DuPont) WO 98/30609, 1998. (e) Pietsch, J.; Braunstein, P.; Chauvin, Y. *New J. Chem.* **1998**, *22*, 467–472. (f) Younkin, T. R.; Connor, E. F.; Henderson, J. I.; Friedrich, S. K.; Grubbs, R. H.; Bansleben, D. A. *Science* **2000**, *287*, 460–462. (g) Rachita, M. J.; Huff, R. L.; Bennett, J. L.; Brookhart, M. *J. Polym. Sci. Part A* **2000**, *38*, 4627–4640. (h) Hicks, F. A.; Brookhart, M. *Organometallics* **2001**, *20*, 3217–3219. (i) Soula, R.; Broyer, J. P.; Llauro, M. F.; Tomov, A.; Spitz, R.; Claverie, J.; Drujon, X.; Malinge, J.; Saudemont, T. *Macromolecules* **2001**, *34*, 2438–2442. (j) Gibson, V. C.; Tomov, A.; White, A. J. P.; Williams, D. *J. Chem. Commun.* **2001**, 719–720. (k) Hicks, F. A.; Jenkins, J. C.; Brookhart, M. *Organometallics* **2003**, *22*, 3533–3545. (l) Connor, E. F.; Younkin, T. R.; Henderson, J. I.; Waltman, A. W.; Grubbs, R. H. *Chem. Commun.* **2003**, 2272–2273. (m) Zuideveld, M. A.; Wehrmann, P.; Röhr, C.; Mecking, S. *Angew. Chem., Int. Ed.* **2004**, *43*, 869–873. (n) Speiser, F.; Braunstein, P.; Saussine, L. *Acc. Chem. Res.* **2005**, *38*, 784–793. (o) Zhang, L.; Brookhart, M.; White, P. S. *Organometallics* **2006**, *25*, 1868–1874. (p) Kuhn, P.; Sémeril, D.; Jeunesse, C.; Matt, D.; Neuburger, M.; Mota, A. *Chem.—Eur. J.* **2006**, *12*, 5210–5219. (q) Göttker-Schnetmann, I.; Wehrmann, P.; Röhr, C.; Mecking, S. *Organometallics* **2007**, *26*, 2348–2362. (r) Yu, S.-M.; Berkefeld, A.; Göttker-Schnetmann, I.; Müller, G.; Mecking, S. *Macromolecules* **2007**, *40*, 421–428. (s) Bastero, A.; Göttker-Schnetmann, I.; Röhr, C.; Mecking, S. *Adv. Synth. Catal.* **2007**, *349*, 2307–2316. (t) Guironnet, D.; Rünzi, T.; Göttker-Schnetmann, I.; Mecking, S. *Chem. Commun.* **2008**, 4965–4967. (u) Wehrmann, P.; Mecking, S. *Organometallics* **2008**, *27*, 1399–1408. (v) Lavanant, L.; Rodriguez, A.-S.; Carpentier, J.-F.; Jordan, R. F. *Organometallics* **2008**, *27*, 2107–2117. (w) Rodriguez, B. A.; Delferro, M.; Marks, T. J. *Organometallics* **2008**, *27*, 2166–2168. (x) Zhou, X.; Bontemps, S.; Jordan, R. F. *Organometallics* **2008**, *27*, 4821–4824.
- (11) (a) Keim, W.; Kowaldt, F. H.; Goddard, R.; Krüger, C. *Angew. Chem., Int. Ed. Engl.* **1978**, *17*, 466–467. (b) Keim, W. *Chem. Ing. Tech.* **1984**, *56*, 850–853. (c) Vogt, D. In *Aqueous-Phase Organometallic Chemistry*; Cornils, B., Herrmann, W. A., Eds.; Wiley-VCH, Weinheim, 1998; pp 541–547.
- (12) (a) Bauers, F. M.; Mecking, S. *Angew. Chem., Int. Ed.* **2001**, *40*, 3020–3022. (b) Soula, R.; Novat, C.; Tomov, A.; Spitz, R.; Claverie, J.; Drujon, X.; Malinge, J.; Saudemont, T. *Macromolecules* **2001**, *34*, 2022–2026. (c) Göttker-Schnetmann, I.; Korthals, B.; Mecking, S. *J. Am. Chem. Soc.* **2006**, *128*, 7708–7709. Review: (d) Mecking, S. *Colloid Polym. Sci.* **2007**, *285*, 605–619.

- (13) Stability of Ni(II) and Pd(II) cationic diimine alkyl complexes toward water: (a) Svejda, S. A.; Johnson, L. K.; Brookhart, M. *J. Am. Chem. Soc.* **1999**, *121*, 10634–10635, see Supporting Information. (b) Held, A.; Mecking, S. *Chem.—Eur. J.* **2000**, *6*, 4623–4629. (c) Berkefeld, A.; Mecking, S. *Angew. Chem., Int. Ed.* **2006**, *45*, 6044–6046. Of neutral phosphinosulfonate Pd(II) complexes. (d) Claverie, J. P.; Goodall, B. L.; Skupov, K. M.; Marella, P. R.; Hobbs, J. *Polym. Prepr.* **2007**, *48*, 191–192.
- (14) Reports of ethylene-acrylate and -methacrylate copolymerizations: (a) Johnson, L. K.; Bennett, A. M. A.; Dobbs, K. D.; Ionkin, A. S.; Ittel, S. D.; Wang, Y.; Radzewich, C. E.; Wang, L. WO 01/92347, 2001. (b) Gibson, V. C.; Tomov, A. *Chem Commun.* **2001**, 1964–1965. Incorporation of MMA exclusively as end groups in enolate-terminated polyethylenes was observed in this work. (c) Wang, L.; Hauptman, E.; Johnson, L. K.; McCord, E. F.; Wang, Y.; Ittel, S. D. WO 01/92342, 2001. (d) Connor, E. F.; Younkin, T. R.; Henderson, J. I.; Hwang, S.; Grubbs, R. H.; Roberts, W. P.; Litzau, J. *J. Polym. Sci. Part A* **2002**, *40*, 2842–2854. (e) Shen, H.; Goodall, B. L. US 2006/0270811, 2006. (f) Rodriguez, B. A.; Delferro, M.; Marks, T. J. *J. Am. Chem. Soc.* **2009**, *131*, 5902–5919.

Scheme 1. Preparation, Catalytic Activity, and Dynamics of **3**

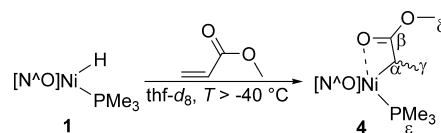
the use of thf as a solvent and an excess of the hydride donor NaHB(OMe)₃ is a prerequisite. The utilization of isolated **1** allows for working in other solvents, such as CD₂Cl₂. Both techniques were used, and no difference in the reactivity of **1** toward the olefinic substrates (see below) was observed either in the absence or presence of the hydride donor NaHB(OMe)₃, which does not react with both the substrates and the organometallic species formed. Characteristic ¹H NMR doublet resonances of **1** were observed at 8.01 (⁴J_{H-P} = 8.7 Hz, -CH=N-), 1.26 (²J_{H-P} = 10.5 Hz, [(N[∧]O)Ni(H)(PMe₃)]), and -26.84 ppm (²J_{H-P} = 143 Hz, [(N[∧]O)Ni(H)(PMe₃)]) in thf-*d*₈ solution.

The higher Ni(II) alkyl complex [(N[∧]O)Ni(CH₂CH₃)(dmsO)] (**3**) was generated by reacting the neutral Ni(II) methyl complex (**2**) with excess ethylene at *T* = 55 °C in dmsO-*d*₆ solution (Scheme 1).^{15b}

Complex **3** catalyzes the dimerization of ethylene to butenes under these conditions. Since solutions of **3** gradually decompose at ambient temperatures, only freshly prepared samples of **3** were used for the studies reported here. Characteristic resonances of **3** are observed at -0.42 (broad quartet, ³J_{H-H} = 7.5 Hz, [(N[∧]O)Ni(CH₂CH₃)(dmsO)]) and -0.07 ppm (broadened triplet, ³J_{H-H} = 7.5 Hz, [(N[∧]O)Ni(CH₂CH₃)(dmsO)]) at 25 °C. Notably, complex **3** undergoes isomerization of the α-methylene and β-methyl protons of the Ni(II)-CH₂CH₃ fragment via the reversible sequence of β-hydride elimination to form an intermediate Ni(II) olefin-hydride species, olefin rotation, and reinsertion.^{15b}

Reaction of Ni(II) Hydride **1** with Polar Vinyl Monomers.

The addition of substoichiometric to small excess amounts of MA (0.8–2 equiv) into a thf-*d*₈ solution of **1** resulted in no observable insertion reaction according to ¹H and ¹³C NMR spectra at temperatures *T* < -40 °C.¹⁷ Warming of the reaction mixture to temperatures *T* ≥ -40 °C in the NMR probe resulted in the gradual consumption of free MA and the stepwise growth of a set of ¹H NMR resonances of a new organometallic species. No changes of either chemical shifts or line widths of the

Scheme 2. Insertion of MA into the Ni(II) Hydride Complex **1**

resonances of the starting reactants were observed in both ¹H and ¹³C NMR spectra, which would indicate reversible binding interactions of MA and the Ni(II) hydride species prior to insertion. Characteristic ¹H NMR resonances of the new organometallic species were observed at -0.16 (H_γ, doublet, ³J_{H_γ-H_α} = 7.4 Hz) and 0.98 ppm (doublet, ²J_{H-P} = 11 Hz, PMe₃) (Figures S2 and S3 in Supporting Information). The ³¹P NMR spectra showed a single resonance at -10.7 ppm. Comprehensive 2D NMR spectroscopic analysis provided the assignment of the organometallic species as **4** (Scheme 2), revealing the H_α resonance as a broad multiplet at 0.91 ppm, which is partly obscured by the intense resonance of the coordinated trimethylphosphine, and which couples to the methyl protons at the γ-carbon atom and the PMe₃ ligand, ³J_{H-P} ≈ 6 Hz (Figure S6).

Insertion of MA had occurred in a 2,1-fashion into the Ni(II) hydride bond exclusively, affording a C-bound¹⁸ Ni(II) alkyl fragment, which bears the methyl ester moiety at the α-carbon. ¹³C NMR spectra (Figure S5) showed characteristic carbon-

(15) (a) Jenkins, J. C.; Brookhart, M. *J. Am. Chem. Soc.* **2004**, *126*, 5827–5842. (b) Berkefeld, A.; Mecking, S. *J. Am. Chem. Soc.* **2009**, *131*, 1565–1574.

(16) Waltman, A. W.; Younkin, T. R.; Grubbs, R. H. *Organometallics* **2004**, *23*, 5121–5123.

(17) A severe broadening of the resonances of the olefinic protons in the ¹H NMR and of the olefinic and carbonyl resonances in the ¹³C NMR spectra was observed upon warming an in situ generated sample of **1** in the presence of substoichiometric to small excess amounts of MA to temperatures -60 °C ≤ *T* ≤ -40 °C in thf-*d*₈ solution. Neither insertion nor hydrogen–deuterium scrambling was observed after the addition of a mixture of deuterium labeled 2,3,3-*d*₃-MA and unlabeled MA under these conditions. Samples of isolated **1** in thf-*d*₈ and CD₂Cl₂ solution did not show this behavior. However, no differences were observed concerning the formation and decomposition of organometallic products.

(18) One could speculate whether complex **4** undergoes isomerization into the κ¹-O bound enolate complex [(N[∧]O)Ni(OC(OMe)CH₂CH₃)(PMe₃)].¹⁶ In light of the scalar coupling observed between the α-methylene and the γ-methyl protons of **4** (³J_{H-H} = 7.4 Hz), the rate of isomerization is expected to be slow enough to be observed by NMR spectroscopy. However, no characteristic resonances attributable to an Ni(II) enolate species were observed in the NMR spectra, suggesting that isomerization either does not occur, or that the equilibrium concentration of the O-bound isomer is too small to be detected.

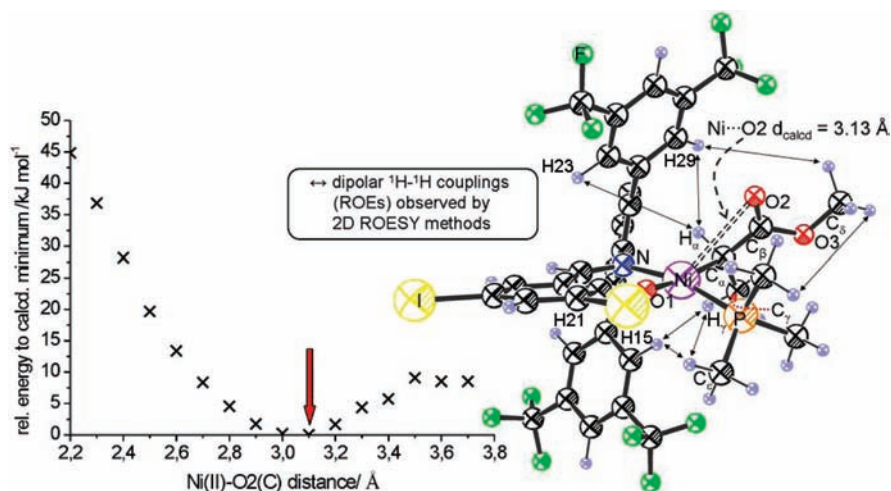


Figure 1. Geometry-optimized structure of **4** obtained from ab initio DFT calculations and relative energy with respect to the minimum structure as a function of the Ni(II)–O₂ distances from 3.7 to 2.2 Å at 0 K in vacuum; calculated Ni(II)–oxygen distance at minimum (marked by red arrow) $d_{\text{calcd}} = 3.13$ Å. Relative proton–proton orientations found are in agreement with dipolar interactions (ROEs, ↔) observed by 2D ROESY (Figure S7, Supporting Information). Selected bond lengths in Å: Ni–P, 2.227; Ni–O₁, 1.950; Ni–N, 1.981; Ni–C_α, 1.998; Ni–H_α, 2.362; C_α–C_β, 1.499; C_β–O₂, 1.233; C_β–O₃, 1.381. Angles: Ni–C_α–H_α, 94.8°; N–Ni–P, 165.6°. Distance of phosphorus to calculated mean square plane defined by C_α, N, Ni, O₁ ≈ 0.79 Å.

phosphorus couplings for all Ni(II) alkyl carbon nuclei and 2D ROESY data revealed a dipolar coupling between the methyl protons H_γ and the PMe₃ protons (Figure S7), which proves that the PMe₃ ligand coordinates to the Ni(II) center. The full ¹H, ¹³C, and ³¹P NMR spectroscopic assignment of **4** is provided in the Supporting Information.

Notably, 2D ROESY data allowed stereospecifically assigning the relative orientations of the α-methine, δ-methoxy, and γ-methyl protons, as well as the trimethylphosphine ligand, by analysis of the distinct dipolar couplings (ROEs, ↔) observed between the functionalized Ni(II) alkyl fragment and the diastereotopic ortho protons (H₂₃, 29 and H₁₅, 21; for numbering see eq 1) Ar-(H)C=N-2,6-{3,5-(F₃C)₂C₆H₃}₂C₆H₃ of the terphenylaniline moiety (Figure S7). The γ-methyl protons and the protons of the PMe₃ ligand point toward the same side of the coordination plane around the nickel center (↔ H₁₅, 21) whereas the α-methine and δ-methoxy protons are oriented toward the opposite side (↔ H₂₃, 29). According to 2D ROESY data, no rotation occurs around the Ni(II)–C_α and C_α–C_β bonds, which suggest interactions between the Ni(II) center and the carbonyl oxygen atom of the functionalized alkyl fragment. Notably, no chemical exchange of the diastereotopic phenyl rings was observed, that is, no rotation occurs around the N–Ar bond.¹⁹ The ¹³C NMR chemical shift of the carbonyl β-carbon is of particular interest as ¹³C and ¹H–¹³C-gHMBC NMR spectra revealed a significant downfield shift by 17.5 ppm vs free MA (166.8 ppm) to 184.3 ppm (doublet, ³J_{C–P} = 8 Hz) (Figure S3), suggesting interactions between Ni(II) and the carbonyl-oxygen atom of the ester moiety.^{20,21}

Ab initio calculations at the gradient-corrected DFT (BP86/LACPV*) level of theory were carried out on the molecular structure of **4**. The results support the structural assignments derived from 2D ROESY data. The question whether favorable interactions between nickel and the carbonyl-oxygen atom may

occur was particularly addressed calculating stationary points on the potential energy surface for Ni(II)–O₂ distances from 3.7 to 2.2 Å in steps of 0.1 Å (Figure 1).²² Relative proton–proton orientations found in the geometry-optimized structure are in agreement with the dipolar proton–proton couplings (ROEs) observed by 2D ROESY, that is the relative orientation of H_α and of γ-methyl and PMe₃-protons, respectively, toward opposite sides of a mean square plane defined by the atoms C_α, N, Ni, O₁. Notably, the calculations indicate a very weak interaction between Ni(II) and the carbonyl-oxygen atom, the obtained interatomic distance of 3.13 Å equals the sum of van der Waals radii of nickel and oxygen (3.15 Å). A calculated distance Ni–H_α of 2.36 Å and angle Ni–C_α–H_α of 95° suggest an

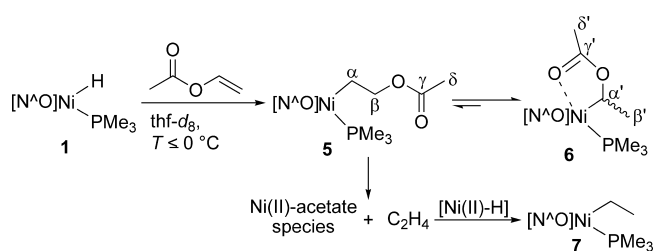
(20) Reports on the chelate nature of polar functionalized Ni(II) alkyls are rare and limited to studies of cationic Ni(II) methyl diimine complexes reacting with the polar vinyl monomers MA and VA. Diethyl ether was displaced from precursor species [(diimine)Ni(CH₃)(OEt₂)]⁺ in the presence of 2 equiv of VA affording a 9:1 mixture of the η²-olefin and η¹-C(O)-bound complexes, respectively. 2,1- and 1,2-insertion of VA into the Ni(II)–methyl bond yielded 5- and 6-membered Ni(II) chelates. The carbonyl ¹³C NMR chemical shift of the 2,1-insertion product was observed at 187.8 ppm. In contrast to VA, the formation of the corresponding η²-olefin and η¹-C(O)-bound complexes was not observed for MA. MA insertion was reported to occur at –40 °C in a 2,1-fashion exclusively, yielding a 4-membered Ni(II) chelate complex that slowly rearranged into the 6-membered chelate complex within the course of one day at room temperature. The low rate of isomerization was attributed to a strong interaction of the electrophilic nickel center and the carbonyl-oxygen atom of the ester moiety. For the four membered chelate [(diimine)Ni(CHMeC(O)OMe)], prepared by protonation of the olefin complex [(diimine)Ni(H₂C=CHC(O)OMe)], low-field NMR signals at 178.2, 177.0, and 174.1 ppm were assigned to C(O)OMe and N=C=N [6, 33] and Brookhart, M.; Johnson, L. K.; Killian, C. M.; Wang, L.; Yang, Z.-Y. US Pat. 5880323, 1999 (example 395).

(21) A series of experiments was carried out with the electron-deficient 1,1-dihydro-pentadecafluorooctyl acrylate (FOA) under otherwise identical conditions. The carbonyl β-¹³C resonances of the organometallic products **4** and **4**_{FOA} only differed by 2.6 ppm. Compared to free FOA (164.8 ppm), the carbonyl resonance shifted by 16.9 ppm to lower fields and was observed as a doublet resonance at 181.7 ppm (³J_{C–P} = 7 Hz).

(22) The nature of the stationary point found as the relative energetic minimum on the potential energy surface was verified by calculating the Hessian matrix, revealing only small imaginary modes <i>ci</i>20 cm⁻¹ that correspond to rotations of the CF₃ groups (see the Experimental Section for details).

(19) The corresponding dipolar couplings to all the aromatic ligand ortho-protons were detected for both the α-methylene and β-methyl protons of the Ni(II)–ethyl complex **3**, indicating free rotation around the Ni(II)–C_α, C_α–C_β, and N–Ar bond in **3**, as opposed to the restricted rotation in **4**. The interconversion of C_α and C_β moieties of **3** occurs at a rate similar to that of the magnetization transfer via dipolar ¹H–¹H couplings (ROEs).

Scheme 3. Insertion of VA into the Ni(II) Hydride 1



α -agostic interaction. The coordination sphere around nickel is slightly tetrahedrally distorted.

Vinyl acetate (VA), together with acrylates, is one of the most important polar-substituted vinyl monomers. Note that, in contrast to MA, there is no precedent of a successful late transition metal catalyzed copolymerization of vinyl acetate with apolar olefins.²³ The addition of VA (2.4 equiv) to a thf solution of **1** (16.6 mM) resulted in no observable insertion reaction at temperatures $T < -20$ °C. Temporary warming of the sample to 0 °C in the NMR probe resulted in a partial reaction of **1** with VA to form a new organometallic species. Rapid cooling to -40 °C allowed its characterization as the 1,2-insertion product **5** (Scheme 3, Figures S8 and S9). Characteristic resonances were observed at 3.82 (broad multiplet, Ni(II)–CH₂CH₂OAc), 1.79 (Ni(II)–CH₂CH₂OC(O)CH₃) and -0.53 ppm (broad multiplet, Ni(II)–CH₂CH₂OAc), consistent with the formation of the 1,2-insertion product of VA (Scheme 3). DQF-COSY data revealed an active coupling of the α - and β -methylene protons of $^3J_{\text{H-H}} \approx 9$ Hz, a passive coupling constant of $^3J_{\text{H-P}} \approx 7$ Hz was observed for the α -methylene protons originating from the ^1H – ^{31}P -coupling to the PMe₃ ligand (Figure S8),²⁴ which was observed at -5.6 ppm in the ^{31}P NMR spectrum. ^1H – ^{13}C -gHMBC spectroscopy revealed the carbonyl ^{13}C NMR resonance of **5** at 170.7 ppm, shifted by only 2.3 ppm to lower field as compared to free VA (168.4 ppm).

NMR spectroscopic monitoring of VA insertion at $T = -10$ °C revealed that complex **5** is the kinetic product, which, aside from its gradual decomposition via β -acetate elimination (see below), rearranges into the thermodynamically favored 2,1-insertion product **6** (Scheme 3). Characteristic resonances of **6** were detected at 4.98 (q, $^3J_{\text{H-H}} = 6.8$ Hz, H $_{\alpha}$), 1.84 (s, H $_{\delta}$), 1.05 (d, $^2J_{\text{H-P}} = 10.5$ Hz, PMe₃), and 1.03 ppm (d, $^3J_{\text{H-H}} = 6.8$ Hz, H $_{\beta}$) (Figures S8 and S10). Coincidentally, the ^{31}P NMR chemical shift of **6** was found to be identical with that of **5**, and was observed at -5.6 ppm. Notably, the ^{13}C NMR chemical shift of the carbonyl carbon atom (C $_{\gamma}$) was detected at 186.4 ppm, substantially shifted to lower field ($\Delta\delta = 18$ ppm) by comparison to free VA, as opposed to complex **5** (Figure S10). The 1,2-insertion product **5** was found to undergo gradual β -acetate elimination at -40 °C overnight, yielding free ethylene (observed at 5.38 ppm) that partially reacted with Ni(II)-hydride species to afford the Ni(II) ethyl complex **7**.²⁵

The nature of functionalized Ni(II) alkyl complexes **5** and **6** was further investigated by computational studies. A geometry scan was carried out calculating stationary points on the potential energy surface for Ni(II)–O2 distances from 5.5 to 2.2 Å (step-

width 0.2 Å) for **5** and from 4.8 to 1.9 Å (step-width of 0.1 Å) for **6** (Figures 2 and 3).

The structural features of complex **6** were found to be similar to those of the 2,1-MA-insertion product **4**. The Ni(II)–O2 distance of 2.78 Å is considerably shorter by comparison to complex **4** (3.13 Å). This value is well below the sum of van der Waals radii of nickel and oxygen (3.15 Å). As a consequence, the coordination sphere around Ni(II) is more tetrahedrally distorted than in **4**. Albeit interactions between Ni(II) and the carbonyl-oxygen are weak they seem more favorable in the case of 5-membered structures than for 4-membered structures as observed for complex **4**. A calculated distance Ni–H $_{\alpha}$ of 2.39 Å and angle Ni–C $_{\alpha}$ –H $_{\alpha}$ of 99° suggest an α -agostic interaction also in **6**. Comparison of the computational data obtained for complex **6** with the experimental and theoretical data of complex **4** suggests a similar relative orientation of the functionalized Ni(II) alkyl fragment in the coordination sphere of the Ni(II) center. Computational studies on **5** revealed a global minimum structure at a Ni(II)–O2 distance of 4.9 Å, which is well above the sum of nickel and oxygen van der Waals radii, and an antiperiplanar orientation of Ni(II) and the β -acyl moiety of the functionalized Ni(II) alkyl fragment.²⁶

Reactivity of Acrylate Insertion Product 4. The polar functionalized Ni(II) alkyl complex **4** was observed to undergo decomposition in the presence of unreacted Ni(II) hydride **1**, affording the saturated ester methyl propanoate.²⁷ The overall rate at which complex **4** decomposes was found to depend on its relative concentration to that of **1**. Monitoring of the progress of the reaction of MA (140 mM) with **1** (52 mM) in thf solution by ^1H NMR showed that the formation of **4** and its decomposition occur simultaneously even at $T = -20$ °C. The ratio of the relative amounts of insertion product **4** and its decomposition product methyl propanoate was found to be <1 throughout the reaction, suggesting similar rates for both reactions at this temperature. No further methyl propanoate formation was observed after complete consumption of **1** (final product ratio of methyl propanoate/**4** $\approx 1.5:1$, Figure S4 and S6), and solutions of **4** free of **1** were found to be stable for days at temperatures $T \leq -30$ °C. Even the addition of a small excess of water (ca. 10 equiv) did not cause decomposition of **4**, ruling out a hydrolytic pathway under these conditions. The undesired decomposition reaction of **1** and **4** is effectively retarded if the starting concentration of **1** is substantially reduced. ^1H NMR spectroscopic monitoring showed that **1** reacted with MA (12.3 mM each) overnight at low temperatures, $T \approx -40$ °C, without noticeable decomposition to afford the desired insertion product **4**.

In preceding mechanistic studies we reported that nonfunctionalized Ni(II) alkyls undergo bimolecular elimination reac-

(23) Terpolymerization of CO, ethylene, and VA with an in situ formed cationic Pd(II) catalyst system based on bidentate phosphorus ligands afforded an alternating CO–olefin (olefin = ethylene, VA) copolymer with a VA incorporation of up to 1.5 mol %. No adjacent ethylene and VA units were observed: Drent, E. EP 0251373 B1, 1992.
(24) For comparison, a ^1H – ^{31}P coupling constant $^3J_{\text{H-P}} = 7$ Hz was observed for complex [(N Δ O)Ni(CH₃)(PMe₃)].

(25) The nature of the resulting Ni(II) acetate species, either being monomeric or oligomeric with bridging acetate ligands, could not be addressed as no indicative ^1H , ^{13}C , and ^{31}P NMR resonances could be assigned.

(26) An additional local minimum was found on the potential energy surface at a Ni(II)–O2 distance restrained to 2.8 Å. However, a free geometry-optimization carried out without a restraint on the Ni(II)–O2 distance always resulted in the global minimum structure. The local minimum is ~ 15 kJ/mol higher in energy and separated by a barrier of at least 66 kJ/mol (Ni(II)–O2 = 3.8 Å) from the global minimum (see Figure 3). Assuming that interconversion of the two structures involves the latter stationary point on the potential energy surface, rate constants $k_{\text{local-global}} \approx 7000$ s $^{-1}$ and $k_{\text{global-local}} \approx 17$ s $^{-1}$ can be calculated at $T = 25$ °C, corresponding to an equilibrium ratio of $K_{\text{local-global}} = k_{\text{local-global}}/k_{\text{global-local}} \approx 1:400$.

(27) Analogously, the decomposition of the FOA insertion product **4**_{FOA} yielded 1,1-dihydro-pentadecafluorooctyl propanoate as the ultimate product.

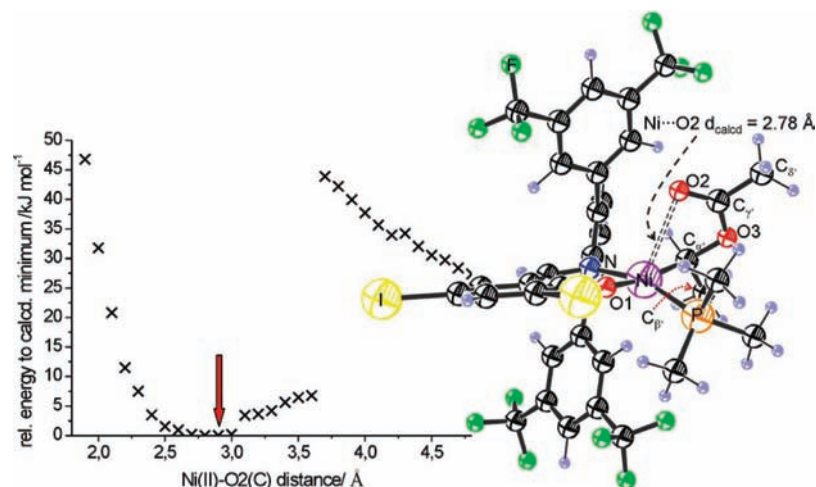


Figure 2. Geometry-optimized structure of **6** obtained from ab initio DFT calculations and relative energy with respect to the minimum structure as a function of the Ni(II)–O2 distances from 4.8 to 1.9 Å at 0 K in vacuum; calculated Ni(II)–oxygen distance at minimum (marked by red arrow) $d_{\text{calcd}} = 2.78$ Å (sum of van der Waals radii of Ni and O = 3.15 Å). Selected bond lengths in Å: Ni–P, 2.224; Ni–O1, 1.959; Ni–N, 1.988; Ni–C $_{\alpha}$, 1.945; Ni–H $_{\alpha}$, 2.387; C $_{\alpha}$ –C $_{\beta}$, 1.520; C $_{\alpha}$ –O3, 1.473; C $_{\gamma}$ –O3, 1.363; C $_{\gamma}$ –O2, 1.228. Angles: Ni–C $_{\alpha}$ –H $_{\alpha}$, 99.4°; N–Ni–P, 161.7°. Distance of phosphorus to calculated mean square plane defined by C $_{\alpha}$, N, Ni, O1 ≈ 0.94 Å.

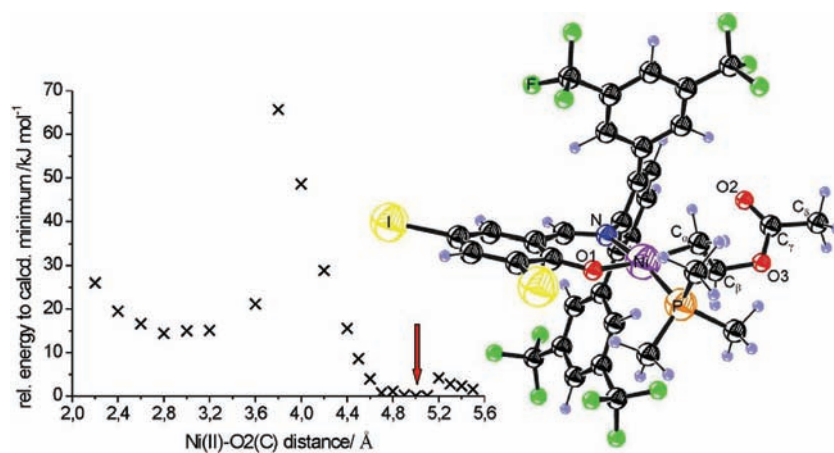
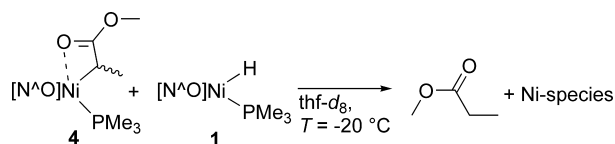


Figure 3. Geometry-optimized structure of **5** obtained from ab initio DFT calculations and relative energy with respect to the minimum structure as a function of the Ni(II)–O2 distances from 5.5 to 2.2 Å at 0 K in vacuum; calculated Ni(II)–oxygen distance at minimum (marked by red arrow) $d_{\text{calcd}} = 5.0$ Å (sum of van der Waals radii of Ni and O = 3.15 Å). Selected bond lengths in Å: Ni–P, 2.210; Ni–O1, 1.959; Ni–N, 1.958; Ni–C $_{\alpha}$, 1.920; C $_{\alpha}$ –C $_{\beta}$, 1.519; C $_{\beta}$ –O3, 1.477; C $_{\gamma}$ –O3, 1.363; C $_{\gamma}$ –O2, 1.225. Angle: N–Ni–P, 171.4°. Distance of phosphorus to calculated mean square plane defined by C $_{\alpha}$, N, Ni, O1 ≈ 0.41 Å.

Scheme 4. Decomposition of Polar Functionalized Ni(II) Alkyl Complex **4** in the Presence of **1**



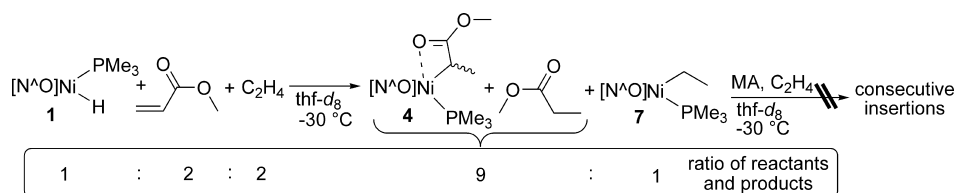
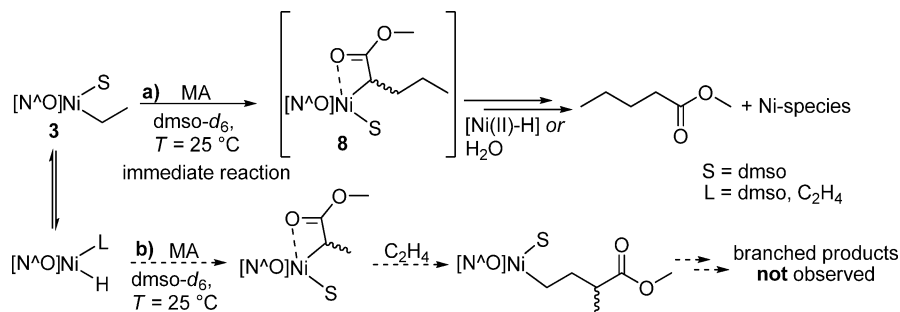
tions with Ni(II) hydrides, affording alkanes as the ultimate decomposition products.²⁸ In agreement with the observed dependence of the overall decomposition rate on the concentration of **1**, a similar bimolecular elimination mechanism for the decomposition of **4** is assumed (Scheme 4).

The stability of **4** in the absence of free Ni(II) hydrides indicates that β -hydride elimination after MA insertion is

unfavorable at low temperatures. **1** (12 mM in CD₂Cl₂ and thf-*d*₈, respectively) reacted with a 2:1 mixture of deuterium-labeled MA-*d*₃ (2,3,3-*d*₃-MA) and MA (a total of 1.4 equiv per [(N \wedge O)Ni(II)-H] species; Figures S2 and S3) to afford the insertion products **4** and **4_D**. Reversible β -hydride or -deuteride elimination from the insertion products **4** or **4_D** would produce reactive Ni(II) hydride and Ni(II) deuteride species that would result in deuterium-hydrogen scrambling between MA and MA-*d*₃ and the γ -methyl moieties of **4** and **4_D**, respectively. No such hydrogen–deuterium scrambling reaction was observed by ¹H NMR spectroscopic monitoring of the reaction progress at –30 °C overnight.²⁹ Also, 2D ROESY data acquired at –20 °C do not indicate chemical exchange between the Ni(II) hydride **1** and the olefinic hydrogens atoms at the 3-position of MA.

Warming a thf-*d*₈ solution of **4** to room temperature (in the absence of free **1**) resulted in gradual degradation to methyl propanoate. Notably, partial isomerization was observed to yield the formal 1,2-MA-insertion product in a 1:10 ratio relative to **4**. Characteristic resonances were detected at 3.42 (Ni(II)–CH₂CH₂C(O)OCH₃), 1.78 (Ni(II)–CH₂CH₂C(O)OCH₃,

(28) The reaction of **1** and **2** yields methane. Activation parameters were determined from linear regression of an Eyring plot (as $\ln(k_{\text{Me-H}}(T))$ vs $1/T$), $\Delta H^\ddagger = (47 \pm 6)$ kJ mol^{–1}, $\Delta S^\ddagger = -(117 \pm 15)$ J mol^{–1} K^{–1}, corresponding to $\Delta G^\ddagger(298\text{K}) = (82 \pm 10)$ kJ mol^{–1}.^{15b}

Scheme 5. Relative Reactivities of Acrylates (MA) and Apolar 1-Olefins (C₂H₄) toward Ni(II) Hydride Species**Scheme 6.** Reactivity of Higher Ni(II) Alkyl Species toward Acrylates, Reaction of **3** and MA

³J_{H-H} ≈ 9 Hz), and -0.55 ppm (Ni(II)-CH₂CH₂C(O)OCH₃, ³J_{H-H} ≈ 9 Hz and ³J_{H-P} ≈ 7 Hz) (Figure S6). Isomerization of **4** involves the formation of the reactive Ni(II) olefin-hydride species [(N^ΛO)Ni(H)(MA)] which either undergoes reinsertion or deactivation in a bimolecular fashion to produce methyl propanoate.

The knowledge of the relative overall reactivity of a polar co-monomer and an apolar olefin toward a reactive metal species is of interest since this factor governs the relative comonomer incorporation in a copolymerization reaction. To this end, Ni(II) hydride complex **1** was reacted with a 2-fold excess of an equimolar mixture of MA and ethylene (1/MA/C₂H₄ ≈ 1:2:2; determined by integration of resonances in ¹H NMR spectra) in the NMR tube. ¹H NMR spectroscopic monitoring showed that ethylene reacted significantly less rapid with **1** to afford the PMe₃-coordinate Ni(II) ethyl complex **7** as compared to MA. Keeping a sample at T = -30 °C for 12 h afforded the Ni(II) alkyls **4** (as the sum of **4** and its decomposition product methyl propanoate) and **7** in an overall ratio of 9:1 (Scheme 5).³⁰

No consecutive insertion reaction of either MA or ethylene with any of the Ni(II) alkyls **4** and **7** was observed under these conditions.

Reactivity of Polar Functionalized Monomers toward Higher Neutral Ni(II) Alkyls. The addition of MA (3.5 equiv rel. to **3**) into a dmsO-d₆ solution of the Ni(II) alkyls **2** and **3** (ratio **2/3** = 1:3) resulted in the immediate consumption of 1 equiv of MA by **3** at room temperature. ¹H NMR spectroscopic monitoring of the reaction progress after MA addition did not

reveal the formation of an organometallic species from MA insertion, but methyl pentanoate was detected as the ultimate reaction product (Scheme 6, pathway a). 2,1-Insertion of MA into the Ni(II)-ethyl bond of **3** yields a short-lived functionalized Ni(II) alkyl species **8**, which is subject to rapid decomposition.

No products from β-hydride elimination after MA insertion into the Ni(II)-ethyl bond, methyl pent-2-enoate (2,1-insertion), or methyl 2-ethyl acrylate (1,2-insertion) were detected in the ¹H NMR spectra. Integration versus an internal standard (anisole) showed that 1 equiv of methyl pentanoate had been formed from **3**, suggesting that the decomposition of the polar functionalized Ni(II) -alkyl species had not occurred preferentially via a bimolecular pathway involving Ni(II) hydride species under the reactions conditions in dmsO solution. In order to further distinguish between a bimolecular deactivation mechanism in the presence of Ni(II) hydride species and a hydrolytic pathway, cross experiments were carried out in which the Ni(II) ethyl complex **3**, and its deuterated analogue **3_D**, were reacted with MA or 2,3,3-*d*₃-MA in dmsO-d₆ solution in the presence of excess D₂O or H₂O, respectively (Scheme 7). Indeed, ¹H NMR spectroscopic monitoring revealed that water (H₂O and D₂O, respectively) acts as a hydrogen source, and incorporation of the aqueous proton (deuteron) had occurred into the 2-position of methyl pentanoate exclusively (Figure S11).³¹ No deuterium incorporation was observed from both the reaction of **3_D** with MA, and of **3** with MA-*d*₃ in the presence of H₂O.

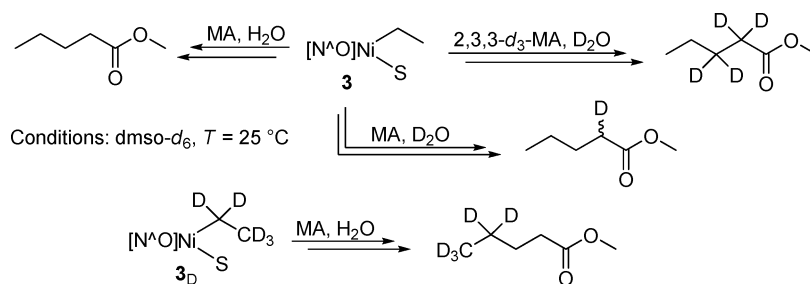
Note that this reactivity toward water of the insertion product (**8**) of MA into the Ni(II)-ethyl bond, by comparison to the inertness of the insertion product (**4**) of MA into the Ni(II)-H bond (see above), certainly also reflects the less labile nature of the PMe₃ ligand in **4** (and the different temperatures required for studies of the two different systems) and does not necessarily indicate a significantly different reactivity of the Ni(II) alkyl substituted at C_α with a methyl vs a propyl group toward water.

Notably, the Ni(II) methyl species was found to undergo much slower reaction with MA by comparison to its Ni(II) ethyl analogue, 1 equiv of linear methyl butanoate was formed over days at room temperature (Scheme 8). This observation qualitatively parallels ¹H NMR spectroscopic studies of the

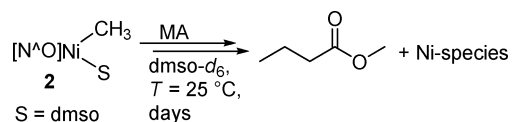
(29) A small (secondary) isotope effect was observed for the overall insertion reaction of 2,2,3-*d*₃-MA and MA with Ni(II) hydride **1**. A 12 mM thf solution of **1** was reacted with 1.4 equiv of a 2:1 mixture of 2,2,3-*d*₃-MA and unlabeled MA at -40 °C overnight, affording the insertion products **4_D** and **4** in a 1:2 ratio (Figure S2). This corresponds to a ratio of the overall insertion rates *r_D*/*r_H* ≈ 0.3. No H-D scrambling was observed under these conditions.

(30) Independent ¹H NMR spectroscopic monitoring of product formation from MA and ethylene insertion into the Ni(II) hydride bond of **1** in thf-*d*₈ solution at -9 °C yielded the second-order rate constants *k*_{ins,NiH,MA} = (21 ± 1)10⁻² M⁻¹ s⁻¹ and *k*_{ins,NiH,C₂H₄} = (1.7 ± 0.1)10⁻² M⁻¹ s⁻¹. According to these kinetic data, the relative reactivity of MA and ethylene toward **1** differs by an order of magnitude which is in agreement with the observed ratio of insertion products **4** and **7** of 9:1.

Scheme 7. Reactivity of Polar Functionalized Ni(II) Alkyls under Aqueous Conditions



Scheme 8. Reactivity of Ni(II) Methyl Species toward Acrylates



reactivity of Ni(II) alkyl complexes **2** and **3** toward ethylene in $\text{dms}\text{-}d_6$ solution.³²

Methyl acrylate (4.4 equiv rel. to $[\mathbf{2}]_{t=0} = 12.7\text{ mM}$) was added to a $\text{dms}\text{-}d_6$ solution of Ni(II) alkyl complexes **2** and **3** in the presence of excess ethylene at $55\text{ }^\circ\text{C}$, that is, under the conditions of an ongoing ethylene dimerization (ethylene was continuously bubbled through the reaction solution from a steel cannula). Acrylate addition resulted in a rapid reaction, as evidenced by an immediate color change from deep red to light orange. Subsequent ^1H , $^1\text{H}-^1\text{H}$ COSY, and ^{13}C NMR spectroscopic analysis of the reaction mixture revealed that **3** had been subject to complete decomposition yielding methyl pentanoate exclusively, while unreacted **2** was the only organometallic species detected.

Surprisingly, VA did not react with both the neutral Ni(II) methyl and the higher Ni(II) alkyl species in $\text{dms}\text{-}d_6$ solution at room temperature. Warming of the sample to $50\text{ }^\circ\text{C}$ resulted in the gradual degradation of **3**, the evolution of ethylene (5.40 ppm) and the gradual growth of a singlet signal at 1.80 ppm, which was tentatively assigned to a Ni(II) acetate species (Scheme 9).

Warming of the sample enhances the formation of reactive Ni(II) hydride species from **3** which react with VA. Presumably, the kinetic insertion product **5*** is formed which is subject to rapid β -acetate elimination (see above).

(31) Orange crystals slowly separated from $\text{dms}\text{-}d_6$ solution upon standing at room temperature. X-ray diffraction revealed the molecular structure as the bischelatate complex $\text{trans}-(\text{N}\Delta\text{O})_2\text{Ni}\cdot 3\text{dms}\text{-}d_6$. The quality of the structure calculation from the diffraction data suffered from the severe disorder of one of the three solvent molecules in the crystal lattice, which could not be resolved. Notably, the coordination sphere around Ni(II) was found to be strongly distorted. Bischelatate complexes have been commonly observed as one ultimate nickel-containing product from decomposition of neutral Ni(II) alkyl species, see reference [10] Hristov, I. H.; DeKock, R. L.; Anderson, G. D. W.; Göttker-Schnetmann, I.; Mecking, S.; Ziegler, T. *Inorg. Chem.* **2005**, *44*, 7806–7818.

(32) A significant difference in the relative reactivity of complexes **2** and **3** was also observed toward ethylene in $\text{dms}\text{-}d_6$ solution at $55\text{ }^\circ\text{C}$; see ref 15b. In more detail, comparison of the ratio of butene vs propene formation (Scheme 1) revealed a higher reactivity of **3** by 1 order of magnitude as compared to **2**. At room temperature, ^1H NMR spectroscopic monitoring showed ethylene consumption to occur slowly and, by comparison of the relative growth of the ^1H NMR resonances of butenes and propene within experimental accuracy, exclusively by **3**.

Summary and Conclusion

Direct NMR spectroscopic observations of organometallic species and decomposition products originating from insertion of polar vinyl monomer into the key intermediates, Ni(II) hydrides and Ni(II) alkyls, of a neutral Ni(II) olefin polymerization catalyst, provide the following insights.

(1) MA readily inserts into the Ni(II)–H moiety of the neutral Ni(II) salicylaldehyde **1** even at low temperature ($-30\text{ }^\circ\text{C}$). Insertion occurs regioselectively to yield the 2,1-insertion product **4** exclusively. The same regioselectivity is also observed for insertion into Ni(II) alkyl species. Low-temperature 2D ROESY demonstrates a weak, but distinct, chelating interaction of the O-atom of the carbonyl group with the Ni(II) center in **4**. A geometry-optimized structure of **4** calculated at the gradient-corrected DFT (BP86/LACVP*) level of theory is in agreement with the structural data obtained from low-temperature NMR spectroscopy.

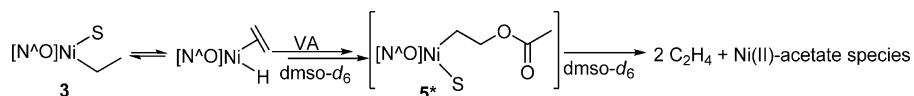
(2) Exposure of the hydride **1** to ethylene and MA at the same time results in the formation of the insertion products of both monomers. This demonstrates that both monomers can effectively compete with one another regarding the net outcome of coordination and insertion, as opposed to a conceivable overwhelming preference for one monomer. Such an effective competition would be one prerequisite for a copolymerization, which appears to be fulfilled.

(3) Decomposition of **4** occurs even at low temperatures by bimolecular reaction with free Ni(II) hydride **1**. In the absence of the latter, **4** is stable at $-40\text{ }^\circ\text{C}$. This requires that no significant (reversible) β -H elimination to intermediate Ni(II)–H species occurs from **4**; the absence of this reaction is indeed supported also by a lack of H/D scrambling between deuterated and nondeuterated MA substrate. At $0\text{ }^\circ\text{C}$, however, β -H elimination does occur to such an extent that decomposition also occurs from solutions containing **4** as the only observable metal species initially, as evidenced by formation of methyl propanoate as the ultimate organic decomposition product.

(4) An additional decomposition pathway is hydrolysis of the Ni(II)–C bond of 2,1-insertion products of MA, in agreement with the previous studies of Grubbs et al.¹⁶ of the organic decomposition products of the reaction of a Ni(II)–phenyl complex, $[(\text{N}\Delta\text{O})\text{NiPh}(\text{PPh}_3)]$, with MA. The system studied allows for a direct comparison of the sensitivity toward hydrolysis with Ni(II) alkyls not bearing a polar substituent ($\text{dms}\text{-}d_6$ solvent, phosphine-free reaction system). Remarkably, while the analogous Ni(II)–Et species is practically stable toward hydrolysis at $55\text{ }^\circ\text{C}$,^{15b} the α -carbonyl substituted metal alkyl originating from 2,1-insertion of MA is subject to rapid hydrolysis at room temperature.

(5) VA inserts less readily into the Ni(II) hydride **1** by comparison to MA insertion. Insertion occurs at $0\text{ }^\circ\text{C}$, yielding both the kinetic 1,2-insertion product (**5**) and the thermodynami-

Scheme 9. Reactivity of VA toward Nonfunctionalized Neutral Ni(II) Alkyls



cally favored 2,1-insertion product (6). NMR data and a theoretical study indicate an interaction of the carbonyl O-atom with the Ni(II) center in 6, structurally similar to the MA insertion product 4. In detail, this interaction appears more pronounced in 6. Decomposition by β -acetate elimination occurs even at low temperatures. Qualitatively, the observed reactivity of VA toward the neutral Ni(II) hydride and alkyls studied parallels observations with cationic Ni(II) diimine complexes³³ regarding the regioselectivity of insertion and β -acetate elimination as a decomposition route.

Throughout this entire study, no further insertion of either ethylene or MA into 4 or evidence of such insertion in other intermittently generated MA insertion products were observed. This appears to be due to a low reactivity of an α -carbonyl substituted metal alkyl for olefin insertion, to which chelate formation, which blocks a coordination site for incoming monomer, may additionally contribute. The challenging nature of copolymerization arises from the combination of this retarded reactivity with the particular susceptibility of functionalized olefin insertion products to specific deactivation reactions, namely bimolecular decomposition with Ni(II) hydride and hydrolytic pathways. An approach to the latter issue is site isolation (and strictly inert conditions), however, enhancing the reactivity of the functionalized olefin insertion product for subsequent insertions also appears to be necessary.

Experimental Section

General Considerations. All manipulations of air- and moisture-sensitive substances were carried out using standard Schlenk, vacuum, and glovebox techniques under argon or nitrogen. Deuterated solvents were purchased from Eurisotop. All solvents were distilled from the corresponding drying agents, thoroughly degassed and saturated with argon prior to use. thf-*d*₈ (99.5 D-%) was dried over a Na/K alloy, dmsO-*d*₆ (>99.96 D-%) over 4 Å molecular sieves or freshly calcined CaO, and CD₂Cl₂ (99.6 D-%) over P₂O₅. Ethylene of 99.95% purity supplied by Gerling Holz + Co was used as received. Ethylene-*d*₄ and 2,3,3-*d*₃-MA (chemical purity >98%, isotope enrichment >99%) supplied by Eurisotop (Cambridge Isotope Laboratories) was used as received. MA, VA, and FOA supplied by Fluka or ABCR were dried over 4 Å molecular sieves, distilled, and thoroughly degassed and saturated with argon prior to use. Technical grade (>90%) sodium trimethoxyborohydride supplied by Sigma Aldrich was washed three times with diethyl ether, dried under high vacuum and stored in a glovebox. The salicylaldimine (N \setminus O)H, 1-C(H)=NAr-2-OH-3,5-I₂C₆H₂ (Ar = 2,6-{3,5-(F₃C)₂C₆H₃}₂C₆H₃)^{10m} and complexes [(N \setminus O)Ni(CH₃)(dmsO)], [(N \setminus O)Ni(C₂H₅)(dmsO)], [(N \setminus O)Ni(Cl)(PMe₃)], and [(N \setminus O)Ni(H)(PMe₃)] were prepared according to known procedures.^{15b} NMR spectra were recorded on a Varian Inova 400 NMR spectrometer. ¹H and ¹³C NMR chemical shifts were referenced to the residual proton and naturally abundant ¹³C resonances of the deuterated solvent. A sample of 85% H₃PO₄ in CDCl₃ was used as an external standard for ³¹P NMR spectra, setting the ³¹P NMR resonance of H₃PO₄ to 0 ppm. Resonances were assigned by ¹H, ¹³C{¹H} and ³¹P NMR spectroscopy, ¹H-¹H-DQF-COSY and ¹H-¹H-ROESY as well as ¹H-¹³C-HSQC and ¹H-¹³C-

gHMBC spectroscopic methods. An overall recycle delay of 7 and 5 s was applied for the collection of ¹H and ¹³C NMR spectroscopic data, respectively. 2D ROESY data were collected with a spin-lock duration of 250 ms at a spin-lock field of 4.40 kHz. In order to prevent TOCSY transfers a 180x-180-x-spin-lock scheme was used. Variable-temperature NMR experiments were carried out with prior temperature determination using a sample of neat methanol (*T* ≤ 40 °C) or ethylene glycol (*T* ≥ 40 °C).

General Procedure for Low-Temperature NMR Studies of the Reactivity of 1 toward Polar Vinyl Monomers. (A) In situ preparation of 1. An NMR tube was charged with 1-Cl and NaHB(OMe)₃ in a 1:3 ratio, sealed with a rubber septum, and removed from the glovebox. After cooling the tube in an isopropanol/dry ice bath to -78 °C, 0.6 mL of thf-*d*₈ were slowly added via syringe and the tube agitated thoroughly to dissolve the solids. The resulting dark brown clear solution was carefully warmed in the cold bath to -10 °C. The progress of formation of 1 was monitored by ¹H NMR spectroscopy at temperatures *T* ≤ -10 °C.

(B) An NMR tube was charged with 1, sealed with a rubber septum, and removed from the glovebox. After cooling the tube in an isopropanol/dry ice bath to -78 °C, 0.6 mL of solvent (thf-*d*₈, CD₂Cl₂, respectively) were slowly added by syringe and the tube agitated thoroughly to dissolve the solid affording clear red to orange solutions.

Concentrations of 1 ranged from 12 to 52 mM. Dry degassed anisole (1.1 μL, 10 μmol) was added into the samples as an internal standard, followed by appropriate amounts of acrylate, VA, and ethylene added with gastight syringes at -78 °C. The cold tubes were briefly agitated and inserted into the NMR probe at the desired temperature. In general, all samples were kept at -78 °C when outside the spectrometer.

Computational Details. The geometries of all complexes were optimized at the gradient-corrected DFT level of theory using the exchange functional of Becke³⁴ in conjunction with the correlation functional of Perdew³⁵ (BP86) and the LACVP* basis set (consisting of an ECP basis set for heavy atoms and of N31G* for all other atoms). Calculations were performed using Jaguar³⁶ (version 5.5.016) running on Linux-2.6.18-4-k7smp on three Athlon64 X2 5600+ dual-core workstations parallelized with MPICH 1.2.4. Crystal structure data of the complex 1-Cl (Figure S1 and Table S1, Supporting Information) were utilized to model the functionalized Ni(II) alkyl complexes 4, 5, and 6, initial structures were obtained by MM+ optimization using Hyperchem.³⁷ Second derivatives (Hessian matrices) were calculated to ensure that true minima were found by showing no large imaginary frequencies (<i>i>20 cm⁻¹) at 298 K.³⁸ All reported energies of geometry-optimized structures were calculated at 0 K in vacuum. Possible chelation was checked by geometry scans calculating stationary points on the potential energy surface for Ni(II)-O2 distances that were varied in steps of 0.1 Å from 3.8 to 2.2 Å and 4.8 to 1.9 Å in the case of 4 and 5, respectively, and in steps of 0.2 Å from 5.5 to 2.2 Å in the case of 6.

(34) Becke, A. D. *Phys. Rev. A* **1988**, *38*, 3098–3100.

(35) Perdew, J. P. *Phys. Rev. B* **1986**, *33*, 8822–8824.

(36) *Jaguar 5.5*; Schrödinger, LLC: Portland, OR, 2003.

(37) *Hyperchem (version 5)*; Hypercube, Inc.: Gainesville, FL.

(38) (a) Krapp, A.; Pandey, K. K.; Frenking, G. *J. Am. Chem. Soc.* **2007**, *129*, 7596–7610. (b) Fan, L.; Ziegler, T. *J. Chem. Phys.* **1992**, *96*, 9005–9012. (c) Fan, L.; Ziegler, T. *J. Phys. Chem.* **1992**, *96*, 6937–6941.

(33) Williams, B. S.; Leatherman, M. D.; White, P. S.; Brookhart, M. J. *Am. Chem. Soc.* **2005**, *127*, 5132–5146.

Acknowledgement. Financial support by the DFG (Me1388/3-2) is gratefully acknowledged. We thank Helmut Fischer for discussions, and Anke Friemel and Ulrich Haunz for technical support. We thank Jannic Wolf for participation in part of this work during his undergraduate studies. S.M. is indebted to the Fonds der Chemischen Industrie and to the Hermann-Schnell Foundation.

Supporting Information Available: Crystal structure data of complex **1-Cl**, comprehensive 1D and 2D NMR spectroscopic data of complexes **4**, **5**, and **6** and decomposition products thereof, and a full list of authors of ref 6c. This material is available free of charge via the Internet at <http://pubs.acs.org>.

JA901360B